





42

43

44

45

### Abstract

46 A multi-model ensemble of Atmospheric Chemistry and Climate Model  
47 Intercomparison Project (ACCMIP) simulations are used to study the atmospheric  
48 oxidized nitrogen ( $\text{NO}_y$ ) deposition over East Asia under climate and emission changes  
49 projected for the future. Both dry and wet  $\text{NO}_y$  deposition shows significant decreases  
50 in the 2100s under RCP 4.5 and RCP 8.5, primarily due to large anthropogenic emission  
51 reduction over both land and sea. However, in the near future of the 2030s, both dry  
52 and wet  $\text{NO}_y$  deposition increases significantly due to continued increase in emissions.  
53 The individual effect of climate or emission changes on dry and wet  $\text{NO}_y$  deposition is  
54 also investigated. The impact of climate change on dry  $\text{NO}_y$  deposition is relatively  
55 minor, but the effect on wet deposition, primarily caused by changes in precipitation, is  
56 much higher. For example, over the East China Sea, wet  $\text{NO}_y$  deposition increases  
57 significantly in summer due to climate change by the end of this century under RCP 8.5,  
58 which may subsequently enhance marine primary production. Over the coastal seas of  
59 China, as the transport of  $\text{NO}_y$  from land becomes weaker due to the decrease of  
60 anthropogenic emissions, the effect of ship emission and lightning emission becomes  
61 more important. On average, seasonal mean total  $\text{NO}_y$  deposition is projected to be  
62 enhanced by 24-48% and 3%-37% over Yellow Sea and East China Sea, respectively,  
63 by the end of this century. Therefore, continued control of both anthropogenic emission  
64 over land and ship emissions may reduce  $\text{NO}_y$  deposition to the Chinese coastal seas.

65

66 Key words: ACCMIP,  $\text{NO}_y$  deposition, RCP 8.5, ship emission

67

68

69

70



## 71 1. Introduction

72 As a nutrient, nitrogen is essential to the terrestrial and marine ecosystems and plays  
73 vital roles in lives on earth from many perspectives such as biodiversity, primary  
74 production, etc. (Doney et al., 2007; Butchart et al., 2010; Stevens et al., 2015;  
75 Galloway et al., 2008). The oceans comprise the largest and most important ecosystems  
76 on Earth and atmospheric nitrogen deposition is an important pathway for delivering  
77 nutrients to the ocean (Duce et al., 2008).

78 The characteristics of atmospheric deposition have been widely studied around the  
79 world. The concentrations and fluxes of trace elements in atmospheric deposition are  
80 influenced by many factors such as rainfall amount, local emissions as well as the long-  
81 range transport of pollutants, etc. (Kim et al., 2000; Cong et al., 2010; Theodosi et al.,  
82 2010; Vuai and Tokuyama, 2011; Kim et al., 2012; Connan et al., 2013; Montoya-  
83 Mayor et al., 2013). Studies have shown significant changes of nitrogen deposition in  
84 the future under the influence of changes in both climate and emissions following the  
85 representative concentration pathways (RCPs) (Van Vuuren et al., 2011; Ellis et al.,  
86 2013; Lamarque et al., 2013a).

87 Since projections of future changes in nitrogen deposition from individual models  
88 are prone to specific model errors (Reichler and Kim, 2008; Shindell et al., 2013), multi-  
89 model ensembles in either climate (Gao et al., 2014; 2016) or chemistry (Lamarque et  
90 al., 2013a; 2013b) are important for identifying robust and non-robust changes  
91 projected by models. This study uses the nitrogen deposition from an ensemble of  
92 models that contributed to the Atmospheric Chemistry and Climate Model  
93 Intercomparison Project (ACCMIP; (Lamarque et al., 2013b)). The nitrogen deposition  
94 includes both the oxidized nitrogen deposition ( $\text{NO}_y$ , mainly including  $\text{NO}$ ,  $\text{NO}_2$ ,  $\text{NO}_3^-$ ,  
95  $\text{N}_2\text{O}_5$ ,  $\text{HNO}_3$  and organic nitrates) and reduced nitrogen ( $\text{NH}_x$ , mainly including  $\text{NH}_3$ ,  
96  $\text{NH}_4^+$  and organic ammonium). Since the number of models with  $\text{NH}_x$  in ACCMIP is  
97 less than 5, this study only focuses on the  $\text{NO}_y$  (10 models or so) deposition, which  
98 mainly results from  $\text{NO}_x$  emissions.



99  
100 Due to the rapid economic development in China, NO<sub>x</sub> emission increase in the past  
101 (Wang et al., 2013) has led to an increase of nitrogen deposition. For example, Liu et  
102 al. (2013) found that nitrogen deposition over land in China increased from 13.2 kg/ha  
103 in 1980s to 21.1 kg ha<sup>-1</sup> in 2000s, with increase of 60%. In addition, the increased NO<sub>x</sub>  
104 emission may also enhance NO<sub>y</sub> deposition in Chinese coastal seas, due to the  
105 atmospheric and riverine transport of NO<sub>x</sub> (Luo et al., 2014). In particular, China has a  
106 long coastline of almost 18,000 km in length and over 300 million square kilometer sea  
107 areas, with high density population and industries in the coastal provinces. Liu et al.  
108 (2016) reported that the shipping NO<sub>x</sub> emissions in East Asia increased from 1.08 Tg  
109 in 2002 to 2.8 Tg in 2013.

110 Studies on the changes of nitrogen deposition under the influence of both climate  
111 and emission changes have been limited over East Asia. Using the old Special Report  
112 on Emissions Scenarios (SRES) such as A2, Lamarque et al. (2005) found large  
113 increases of nitrogen deposition over East Asia due to increased emissions, whereas the  
114 effect from climate change is much smaller and lacks consensus due to the small  
115 ensemble size. In 2100 nitrogen deposition changes due to changes in climate are much  
116 less than changes due to increased nitrogen emissions. In contrast, based on the new  
117 scenarios RCP 4.5 and 8.5, Lamarque et al. (2013a) found that the total NO<sub>y</sub> deposition  
118 (wet + dry; Fig. 5a in Lamarque et al. (2013a)) over East Asia was projected to decrease  
119 by the end of this century due to the combined effect of emissions and climate, but the  
120 changes are mainly triggered by the decrease of emissions. However, the individual  
121 effect of climate or emissions was not examined in that study. With the same dataset of  
122 ACCMIP, Allen et al. (2015) found that by keeping the emissions at current level,  
123 atmospheric aerosol shows significant changes with changing climate, i.e., aerosol wet  
124 deposition decreases over the tropics and Northern Hemisphere midlatitudes with  
125 reduction in precipitation over land. Climate change alone may modulate the changes  
126 in the deposition, particularly for wet deposition due to the response of precipitation to  
127 climate change. Hence, it is important to elucidate the influence of climate and emission  
128 changes on the dry and wet NO<sub>y</sub> deposition over East Asia using the multi-model



129 ensemble ACCMIP results.

130

131 In what follows, we first discuss the capability of ACCMIP in capturing the  
 132 deposition patterns, followed by the changes of dry and wet deposition in future under  
 133 the combined effect of climate change and emissions. Lastly, we elucidate the  
 134 individual effect from climate change or emissions.

## 135 2. Model description

136 In this study, about 10 models from ACCMIP are used, similar to Lamarque et al.  
 137 (2013b). All the data are interpolated to a spatial resolution of  $2^\circ \times 2^\circ$  to facilitate  
 138 analysis and comparison across models. To evaluate the impacts of climate and  
 139 emission change as well as to isolate their individual effect, five cases of ACCMIP  
 140 scenarios are used in this study, as listed in Table 1. The base case over the historical  
 141 period covers the decade of 2000, mainly from 2001-2010. Two cases target the  
 142 investigation of both climate and emission changes under future scenarios of RCP 4.5  
 143 and RCP 8.5, covering two periods in the decades of 2030 and 2100 (first column of  
 144 Table 1). The remaining two cases are used to investigate the impact from climate  
 145 change only in the 2030s and 2100s under RCP 8.5 by maintaining emission at the level  
 146 of year 2000 (last column of Table 1). As different models have different simulation  
 147 years, some model may not cover the entire decades of 2030 and 2100. Detailed  
 148 simulation lengths for each model are listed in Table S1. In the ACCMIP dataset, the  
 149 summation of all simulated oxidized nitrogen species is referred to as  $\text{NO}_y$ , which is the  
 150 major focus of this study.

151 Table 1. Scenarios used in this study

152

	Base	Changes in both climate and emissions		Climate change only	
Scenarios	Historical	RCP 4.5	RCP 8.5	Em2000Cl2030	Em2000Cl2100
Period	2000-2010	2030-2039	2030-2039	2030-2039	2100-2109
		2100-2109	2100-2109		

153



### 154 3. Evaluation of the ACCMIP results

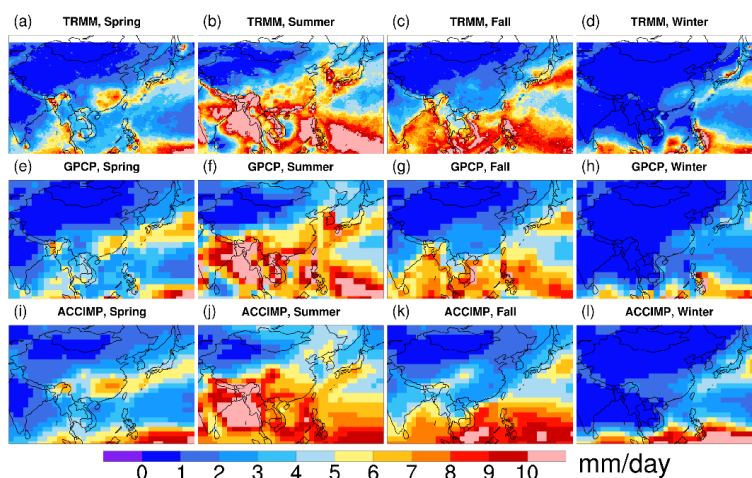
155 The deposition results of ACCMIP have been extensively evaluated previously  
156 across land areas by comparing with three datasets including North American  
157 Deposition Program (NADP), European Monitoring and Evaluation Programme  
158 (EMEP) and Acid Deposition Monitoring Network in East Asia (EANET), and  
159 reasonable performance was demonstrated by the ACCMIP results (Lamarque et al.,  
160 2013a). There is a lack of deposition data over the ocean, making evaluation of the  
161 ACCMIP results across the oceans difficult. Recently, Baker et al. (2017) conducted an  
162 intensive evaluation of the ACCMIP multi-model mean based on a large number of dry  
163 NO<sub>y</sub> deposition samples, i.e., a total of 770 samples collected over the Pacific, showing  
164 comparable spatial distributions between observations and ACCMIP, such as a  
165 consistent northwest-southeast gradient with higher deposition flux closer to the coast  
166 (Fig. 12 in Baker et al. (2017)). In terms of wet deposition, considering the close  
167 relationship between wet deposition and precipitation (Kryza et al., 2012; Wałaszek et  
168 al., 2013), evaluation of precipitation is performed using the Tropical Rainfall  
169 Measuring Mission (TRMM; <http://pmm.nasa.gov/trmm>) and Global Precipitation  
170 Climatology Project (GPCP) v 2.3 (Adler et al., 2018) precipitation data. Fig. 1 shows  
171 a comparison of the annual mean precipitation over the historical period (2000-2010)  
172 among the ACCMIP multi-model ensemble mean and TRMM, which only covers  
173 60°N-60°S, and GPCP. In general, the ACCMIP mean precipitation well captured the  
174 spatial variations of the observed precipitation from both TRMM and GPCP, with  
175 stronger precipitation in the southern part of Asia, particularly over the South China Sea  
176 and the Bay of Bengal, and lighter precipitation in northern China (i.e., Northwest  
177 China). In particular, the rain belt stretching from the east of Japan to the Philippines in  
178 summer is also well captured by ACCMIP.

179

180

181

182



183  
184  
185  
186

Fig. 1. Evaluation of seasonal mean precipitation during 2001-2010: ACCMIP multi-model ensemble mean vs. TRMM and GPCP

#### 187 4. Future changes of NO<sub>y</sub> deposition in East Asia

188 Considering the uncertainty and variability among multiple ACCMIP results, all  
189 analyses, i.e., the future changes of deposition, are performed based on model  
190 agreement and statistical significance. Following our previous studies (Gao et al., 2014;  
191 2015), results at a model grid cell are considered to have agreement if at least 70% of  
192 the ACCMIP models show the same sign of change as the ACCMIP multi-model  
193 ensemble mean. For models showing agreement with the ensemble mean, if more than  
194 half of the models show statistical significance at 95% level, then the ensemble mean  
195 change for that particular grid is considered to be statistically significant.

196 The seasonal mean distribution of dry NO<sub>y</sub> deposition over East Asia areas for  
197 historical (2001-2010) and projected future changes under RCPs scenarios (RCP 4.5  
198 and RCP 8.5) during the two periods of 2030 and 2100 are shown in Fig. 2. The four  
199 seasons defined in this study are spring (March to May), summer (June to August), fall  
200 (September to November) and winter (December to February).

201 As anthropogenic activities play important roles in NO<sub>x</sub> emissions, high

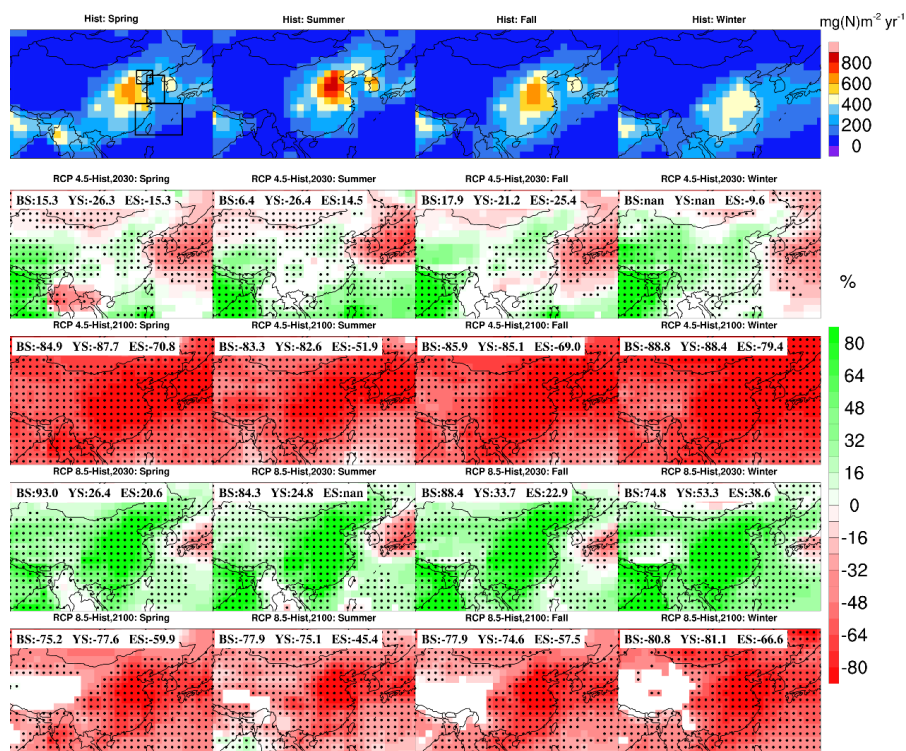


202 atmospheric dry nitrogen ( $\text{NO}_y$ ) deposition values mainly cluster around areas with high  
203 population density and industrial activities in the historical periods (top row of Fig. 2),  
204 e.g., high values of  $\text{NO}_y$  deposition can be seen in East China, Korea, Japan and their  
205 coastal seas. In this study, in addition to the land areas, we also focus on three coastal  
206 seas in East Asia (Bohai Sea, Yellow Sea and East China Sea from high latitude to low  
207 latitude, referred to as the BYE areas below), marked by the three black boxes in Fig.  
208 2a. A gradient of decreasing  $\text{NO}_y$  deposition is found (top row of Fig. 2) from eastern  
209 China to the coastal areas. Seasonal variations show that over mainland China, summer  
210 is the season with the highest dry and wet  $\text{NO}_y$  deposition, with high dry deposition  
211 likely caused by the high deposition velocity (Zhang et al., 2017) and wet deposition  
212 due to larger precipitation in summer, consistent with previous studies (Liu et al., 2017;  
213 Zhang et al., 2017; Xu et al., 2018). Over the ocean such as Yellow Sea and East China  
214 Sea, the notably higher  $\text{NO}_y$  deposition (first row of Fig. 2) is partly attributed to  $\text{NO}_x$   
215 emission transported from land to the coastal seas. In particular, the dry  $\text{NO}_y$  deposition  
216 over the East China Sea is obviously higher in winter compared to summer, likely  
217 resulting from enhanced transport by the northwesterly winds during the winter  
218 monsoon (Ding, 1991).

219 Considering the projected future changes of  $\text{NO}_y$  deposition, we show the  
220 distributions in the 2030s and 2100s under the RCP 4.5 and RCP 8.5 scenarios,  
221 representing near-term and long-term changes. Dry  $\text{NO}_y$  deposition decreases  
222 remarkably in the 2100s under the RCP 4.5 and RCP 8.5 scenarios over East Asia, a  
223 result of large decrease in emissions (second column in Fig. S1 in the supporting  
224 information). In the 2030s, besides the decrease of dry deposition in Japan, Korea and  
225 the surrounding areas, RCP 8.5 shows a predominant increase of dry deposition (Fourth  
226 row in Fig. 2); in contrast, robust significant increases in western China and India are  
227 projected, with little or weak signals in eastern China in RCP 4.5, consistent with the  
228 emission change patterns (first column in Fig. S1).

229

230



231

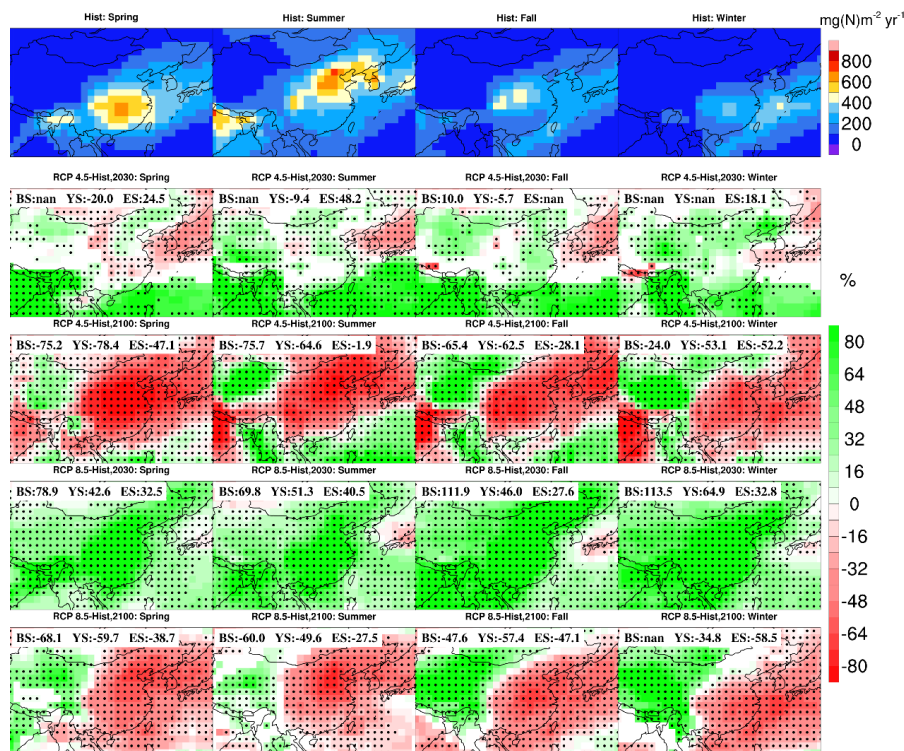
232 Fig. 2 Spatial distribution of mean seasonal dry  $\text{NO}_y$  deposition over East Asia under historical  
 233 (2001–2010; top row) as well as the future changes (second to fifth rows representing changes under  
 234 RCP 4.5 2030, RCP 4.5 2100, RCP 8.5 2030 and RCP 8.5 2100 in relative to historical period). Only  
 235 grids with multi-model agreement are shown (grids without model agreement are in white), and  
 236 stippling marks areas with statistical significance ( $\alpha=0.05$ ). Regions of Bohai Sea (BS), Yellow Sea  
 237 (YS) and East China Sea (ES) are marked by the black rectangles in the top left panel, with mean  
 238 changes shown on the top left of each panel starting from the second row. The mean change of a  
 239 region is set to nan if the number of significant grids in this region is less than half of the area.

240

241 For wet  $\text{NO}_y$  deposition, as discussed earlier, summer is the season with strongest  
 242 deposition (first row of Fig. 3), primarily caused by the largest precipitation among the  
 243 four seasons (Fig. 1). In the 2030s, changes of wet deposition (second and fourth rows  
 244 of Fig. 3) are in general similar to the patterns of dry deposition changes (second and  
 245 fourth rows of Fig. 2). However, in the 2100s, the patterns of wet deposition changes  
 246 are different from those of dry depositions, with relatively clear east/west dipole  
 247 features in particular under RCP 8.5. To elucidate what controls the dipole patterns, the  
 248 individual effect of climate change and emissions is discussed in the next section.



249



250

251

Fig. 3. Same as Fig. 2 except for wet  $\text{NO}_y$  deposition.

252

## 5. The impact of climate change or emissions on $\text{NO}_y$ deposition

253

Two scenarios from ACCMIP are used in this study to isolate the influence of anthropogenic emissions and climate change on  $\text{NO}_y$  deposition. The two scenarios are shown in Table 1, with emissions kept at the current level (the decade of 2000) but climate for the 2030s and 2100s under RCP 8.5 are compared.

257

Climate change alone has negligible contributions to the dry  $\text{NO}_y$  deposition changes, as shown in Fig. 4. Generally, calculation of dry deposition flux in chemical models follows equation 5.1, where  $F$  is vertical dry deposition flux,  $C$  is concentration of specific gas or particle and  $v_d$  is the dry deposition velocity.

261

$$F = -v_d C \quad (5.1)$$

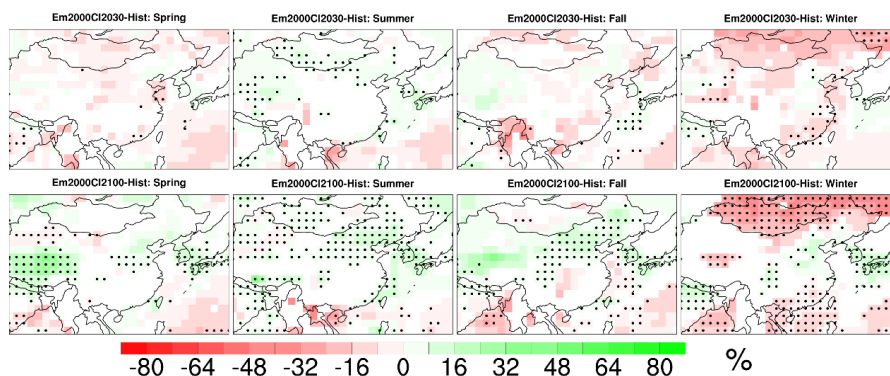


262 All models in ACCMIP calculated dry deposition velocity using the resistance  
263 approach (Lamarque et al., 2013b), which defines the inverse of dry deposition velocity  
264 as equation 5.2,

$$265 \quad \frac{1}{v_d} = r_t = r_a + r_b + r_c \quad (5.2)$$

266 where  $r_t$  is the total resistance,  $r_a$  is the aerodynamic resistance which is common to  
267 all gases,  $r_b$  is the quasilaminar sublayer resistance and  $r_c$  is the bulk surface resistance  
268 (Steinfeld, 1998). As  $r_b$  depends on the molecular properties of the target substance and  
269 deposition surface and  $r_c$  depends on the nature of surface (Steinfeld, 1998), they do not  
270 vary under climate change. As for  $r_a$ , it plays a significant role in transporting gases and  
271 particles from atmosphere to the receptor surface.  $R_a$  is governed by atmospheric  
272 turbulent transport, mainly controlled by the wind shear as well as buoyancy (Erisman  
273 and Draaijers, 2003). Therefore, climate change affects dry deposition velocity for the  
274 gases or particles mainly through its modulation of  $r_a$ . As shown in Fig. 4, the changes  
275 of dry depositions from climate change alone are mostly negligible compared to the  
276 total changes from both climate change and emissions (Fig. 3), indicating statistically  
277 insignificant change of  $r_a$  under a warmer climate.

278

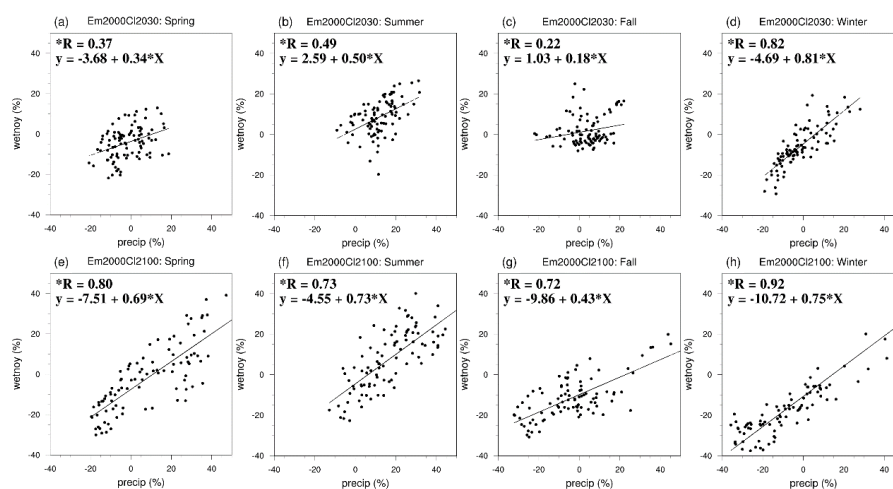


279

280 Fig. 4. Spatial distribution of mean seasonal dry  $\text{NO}_y$  deposition change over East Asia under  
281 experimental scenarios of ACCMIP (Em2000Cl2030 and Em2000Cl2100) relative to historical  
282 period (2001-2010). The distribution of mean seasonal dry  $\text{NO}_y$  deposition under historical period  
283 is shown in Fig. 2 (top row). Only grids with multi-model agreement are shown (grids without model  
284 agreement are in white), and among the grids with model agreement, stippling marks statistical  
285 significance ( $\alpha=0.05$ ).



286        Considering the impact of climate conditions on  $\text{NO}_y$  deposition, precipitation is an  
287 important factor and has been shown to positively correlate with wet  $\text{NO}_y$  deposition  
288 (Kryza et al., 2012; Wałaszek et al., 2013). In order to further quantify the relationship  
289 between wet deposition and precipitation, we display in Fig. 5 the correlation between  
290 the changes of precipitation and wet  $\text{NO}_y$  deposition over the BYE areas for the  
291 scenarios with fixed emissions. All correlations are positive and statistically significant.  
292 There is a larger inter-model spread of changes in Em2000Cl2100 compared to  
293 Em2000Cl2030, and the larger changes in precipitation and wet deposition allow a  
294 stronger correlation between them to emerge in the 2100s relative to the 2030s.  
295 Meanwhile, winter owns the highest correlation in both Em2000Cl2030 and  
296 Em2000Cl2100, partly related to the significant decrease of both wet  $\text{NO}_y$  and  
297 precipitation in winter under Em2000Cl2100 over East China Sea which will be  
298 discussed in detail next.



299

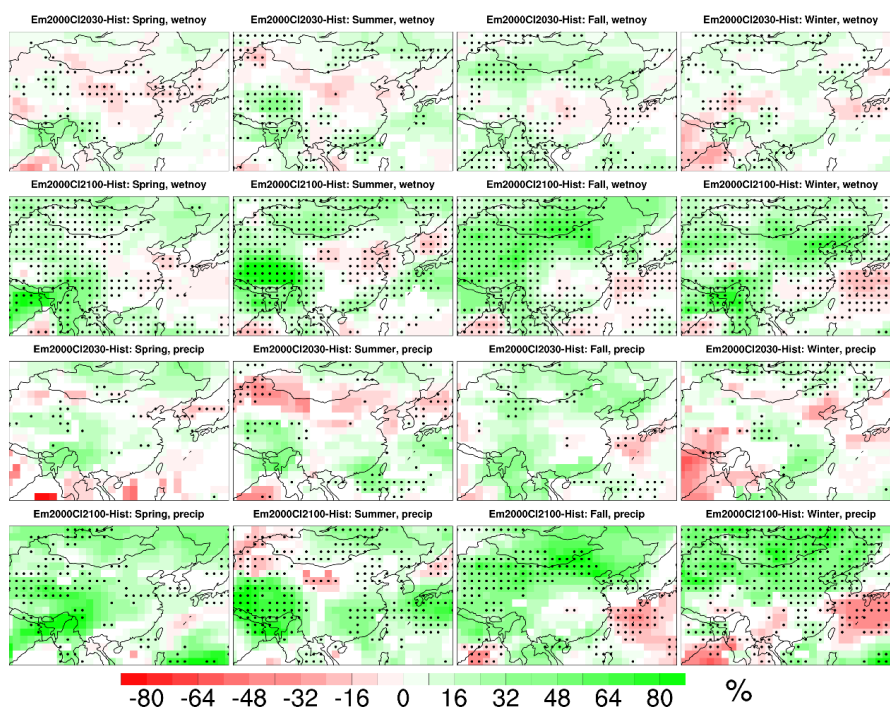
300 Fig. 5. Comparison between precipitation and wet  $\text{NO}_y$  deposition changes under the experimental  
301 scenarios of ACCMIP (Em2000Cl2030 and Em2000Cl2100) relative to historical period (2001-  
302 2010) over Bohai Sea, Yellow Sea and East China Sea. An *t*-test ( $\alpha=0.05$ ) is performed in each panel  
303 for statistical significance and the star before “R” indicates statistical significance at 95% confidence  
304 level. Each point in this figure corresponds to the results from an individual model of ACCMIP.

305

306 As depicted in Fig. 6, the changes of wet deposition in the 2030s due to climate  
307 change is mostly insignificant (first row) and correspond well with the insignificant



308 changes of precipitation (third row). Similarly, the patterns in the 2100s between the  
309 changes of wet deposition (second row) and precipitation (fourth row) are quite  
310 consistent. For example, in spring, summer and fall, a dominant increase in western  
311 China is projected (first three panels in the second and fourth rows), whereas in winter,  
312 a north and southeastern dipole feature is clearly seen. Over the East China Sea, wet  
313  $\text{NO}_y$  deposition increases significantly in summer (18%) and decreases significantly in  
314 winter (-13%), indicating a remarkable influence of climate change on the wet  $\text{NO}_y$   
315 deposition. The changes of precipitation are generally consistent with that reported in  
316 other studies. Both Chong-Hai and Ying (2012) and Wang and Chen (2014) show  
317 significant increase of precipitation except for eastern South China at the end of the 21<sup>st</sup>  
318 century under RCP 8.5. Comparing Fig. 6 with Fig. 3, it is clear that the dipole pattern  
319 of changes in wet deposition in the 2100s shown in Fig. 3 is primarily related to the  
320 large reduction of emission over eastern China.



321

322

323 Fig. 6. Spatial distribution of mean seasonal wet  $\text{NO}_y$  deposition change and precipitation change  
324 under EM2000CI2030 and EM2000CI2100 relative to historical period (2001-2010). The panels are  
325 drawn and arranged in the same manner as Fig. 2.



326 From the global perspective, the emission of nitrogen oxide is in general balanced  
327 by the  $\text{NO}_y$  deposition as documented in Lamarque et al. (2013a) using the ACCMIP  
328 model results, although  $\text{NO}_y$  deposition might be larger due to the downward transport  
329 from the stratosphere. Over the Chinese coastal seas, we calculate the multi-model  
330 seasonal mean  $\text{NO}_y$  deposition and  $\text{NO}_x$  emissions, mainly from ships and lightning. To  
331 avoid biases from spatial interpolation, calculation is performed based on the original  
332 model grid and regionally averaged for each model. Since the changes in Bohai are less  
333 significant in general, particularly in the near future (second row of Figs. 2,3), we only  
334 focus on the emission and deposition changes over Yellow Sea and East China Sea. The  
335 total  $\text{NO}_x$  emissions over the oceans such as Yellow Sea and East China Sea can be  
336 mainly classified into two categories, ship and lightning emissions. As a dominant  
337 contributor of  $\text{NO}_x$  emission in the ocean (Dalsøren et al., 2009; Eyring et al., 2010),  
338 Fan et al. (2016) concluded that 85% of ship emissions took place within 200km of the  
339 coastlines. As reported by Liu et al. (2016), ship emissions from East China Sea may  
340 account for a large percentage (31%) of the total ship emission in East Asia. Thus, ship  
341 emission may contribute significantly to emissions in the Chinese coastal seas. The  
342 percentage of dry and wet deposition, as well as the ratio of ship emission and lightning  
343 emission to the total  $\text{NO}_y$  deposition are shown in Figs. 7 and 8. The ratio of ship  
344 emission and lightning emission to the total  $\text{NO}_y$  deposition is used to characterize their  
345 contribution to  $\text{NO}_y$  deposition with the assumption that all ship and lightning emission  
346 contribute to the  $\text{NO}_y$  deposition, which can be considered an upper bound of their  
347 contribution.

348 A couple of features can be identified from Fig. 7 and Fig. 8. First, the percentage  
349 of dry deposition over Yellow Sea and East China Sea (third and fifth blue color bars  
350 from the left in each panel of Figs. 7, 8) decreases in the 2100s under RCP 4.5 and RCP  
351 8.5, consistent with the patterns shown in Fig. 2 (third and fifth rows), due primarily to  
352 emission reduction. Second, with larger emission reduction over land (e.g., eastern  
353 China) compared to ocean (Fig. S1), the contribution of ship emission to total  $\text{NO}_y$   
354 deposition over the seas may become larger in future (black color bars in Figs. 7,8). For  
355 instance, over the historical period, the seasonal contribution of ship emission to total



356 NO<sub>y</sub> deposition is 22%-30% and 52%-82% for Yellow Sea and East China Sea,  
357 respectively; however, in 2100, it reaches 56%-99% (RCP 4.5) and 42-58% (RCP 8.5)  
358 for Yellow Sea, 81% to almost 100% (RCP 4.5) and 74% to almost 100% (RCP 8.5) for  
359 East China Sea, with mean seasonal increase of 24-48% and 3%-37% for Yellow Sea  
360 and East China Sea, respectively. Third, the contribution of lightning NO<sub>x</sub> in spring and  
361 winter is negligible, however, the contribution is nontrivial in summer and fall. In  
362 particular, due to the reduction in anthropogenic emissions and ship emissions in 2100  
363 under RCP 4.5 and RCP 8.5, the contribution of lightning NO<sub>x</sub> becomes more obvious  
364 compared with the case without emission reduction. For example, in the summer of the  
365 2100s, the contribution of lightning NO<sub>x</sub> increases from 1% to 7% (both RCP 4.5 and  
366 RCP 8.5) over Yellow Sea, 3% to 7% in RCP 4.5 and 6% in RCP 8.5 over East China  
367 Sea. In the fall of the 2100s, the contribution of lightning NO<sub>x</sub> increases from less than  
368 1% to 3% (both RCP 4.5 and RCP 8.5) over Yellow Sea, and 1% to 4% (both RCP 4.5  
369 and RCP 8.5) in East China Sea. These results illustrate a shift in the future towards  
370 enhanced impacts from ship and lightning emissions when anthropogenic emissions are  
371 largely controlled in the upwind land regions.

372

373

374

375

376

377

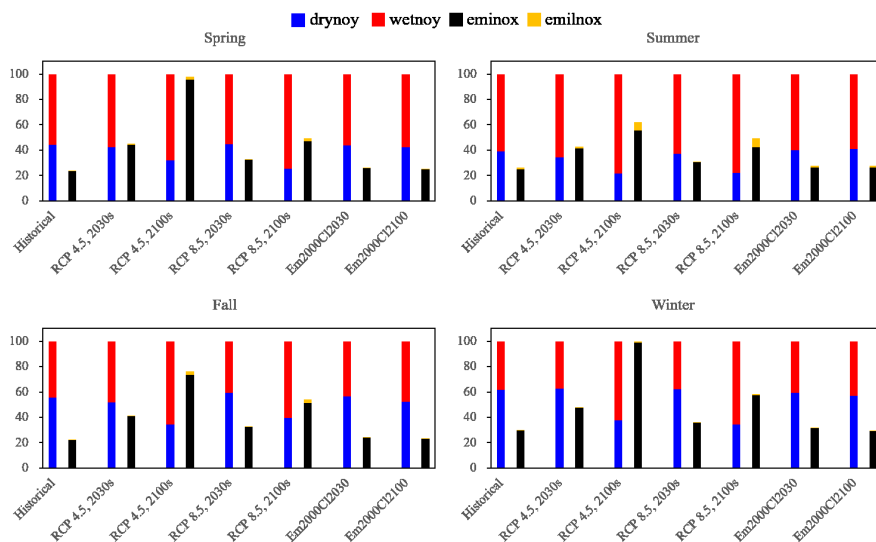
378

379

380

381

382



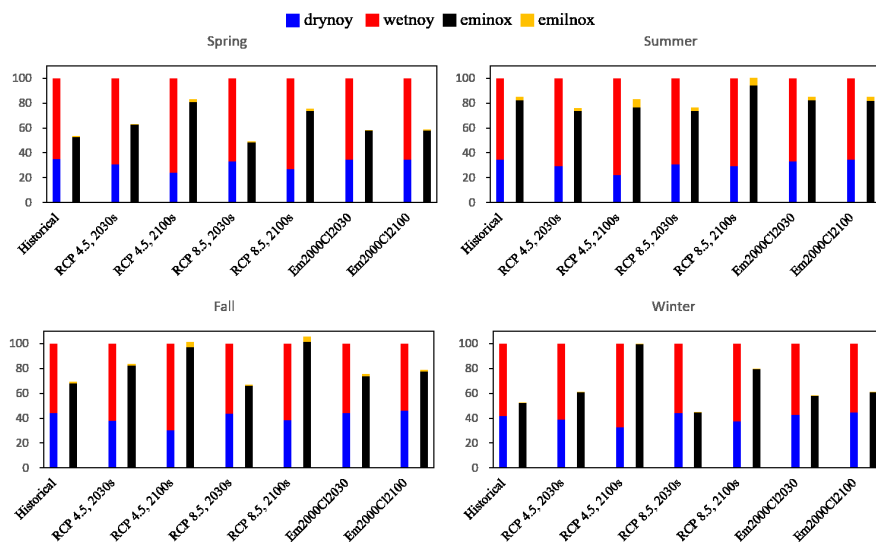
383

384 Fig. 7 Stacked bars of seasonal ratio of NO<sub>y</sub> deposition from wet (wetnoy) and dry  
385 (drynoy) deposition and NO<sub>x</sub> emissions from ship (eminox) and lightning (emilnox) to  
386 the total (wet + dry) NO<sub>y</sub> deposition in the historical and RCP scenarios over Yellow  
387 Sea. Two color bars are shown for each period with the left one representing dry NO<sub>y</sub>  
388 (blue) and wet NO<sub>y</sub> (red) deposition and the right one representing eminox (black) and  
389 emilnox (orange).

390

391

392



393

394

Fig. 8 Same as Fig. 7 except for East China Sea.

## 395 6. Marine primary production over the BYE areas and its future 396 change

397 Generally, the Chinese coastal seas have rich nutrients and high total primary  
 398 production (Gong et al., 2000; Son et al., 2005). Thus, these areas seldom lack nutrient  
 399 but sometimes eutrophication is an environmental issue. For instance, a massive *Ulva*  
 400 *prolifera* bloom occurred in June 2008 in the Yellow Sea and the harmful algal bloom  
 401 caught a lot of attention. Hu et al. (2010) found that algal blooms occur in each summer  
 402 of 2000-2009 in the Yellow Sea and East China Sea. Atmospheric deposition is an  
 403 important source of nutrient for the marine ecosystem, and it can facilitate primary  
 404 production (PP) in the ocean surface and contribute to the development of harmful algal  
 405 blooms (Paerl and Hans, 1997; Paerl et al., 2002).

406 Several previous studies have investigated PP over the BYE areas and estimated the  
 407 historical annual PPs to be  $97\text{gC m}^{-2}\text{ yr}^{-1}$ ,  $236\text{gC m}^{-2}\text{ yr}^{-1}$  and  $145\text{gC m}^{-2}\text{ yr}^{-1}$ ,  
 408 respectively, for Bohai Sea, Yellow Sea and East China Sea (Guan et al., 2005; Gong et  
 409 al., 2003). In this study, based on the assumption that all  $\text{NO}_y$  deposited into surface



410 ocean can be absorbed by phytoplankton, we estimate the model averaged PP from NO<sub>y</sub>  
411 deposition in the historical period over the BYE areas according to the Redfield ratio  
412 (Tett et al., 1985). The Redfield ratio refers to the ratios of carbon, nitrogen and  
413 phosphorus in phytoplankton listed in equation 6.1. Equation 6.2 are used to calculate  
414 PP generated from NO<sub>y</sub> deposition, where PP<sub>noy</sub> represents the PP from NO<sub>y</sub>  
415 deposition and NO<sub>y</sub> represents total NO<sub>y</sub> (wet + dry) deposition.

$$416 \quad C : N : P = 106 : 16 : 1 \quad (6.1)$$

$$417 \quad PP_{noy} = NO_y \times \frac{106}{16} \quad (6.2)$$

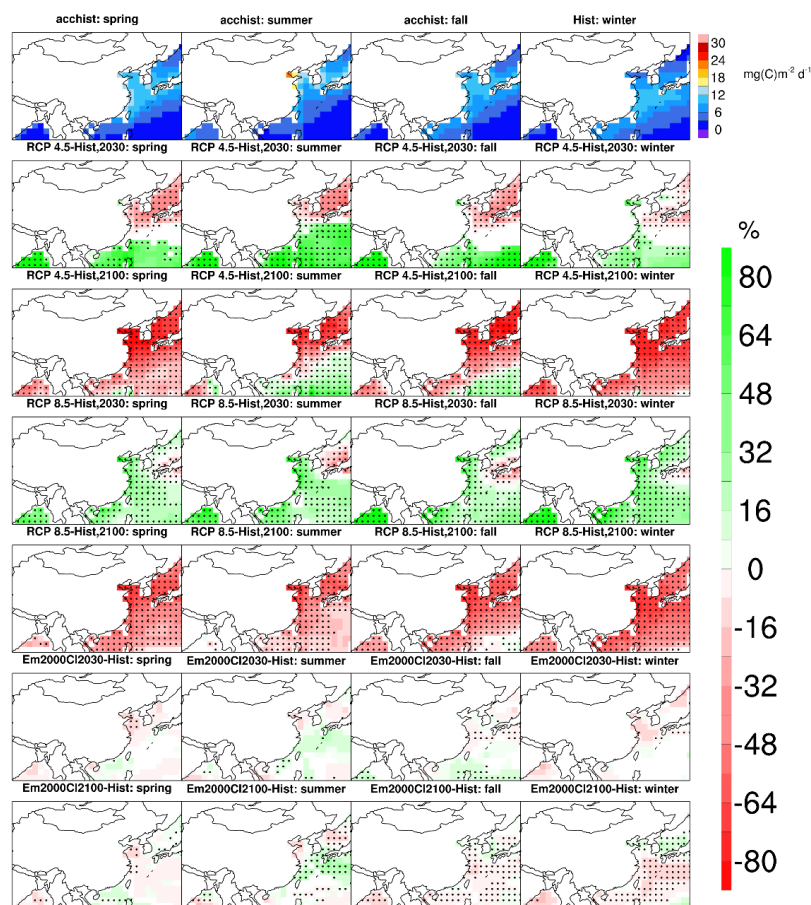
418 Results show that PP from historical NO<sub>y</sub> deposition is 5, 5.4 and 4.4 gC m<sup>-2</sup> yr<sup>-1</sup>  
419 over Bohai Sea, Yellow Sea and East China Sea, accounting for 5%, 2% and 3% of PP  
420 in those three seas, respectively. These values are consistent with a previous study  
421 reported by Qi et al. (2013), which indicated a contribution of 0.3~6.7% to PP from the  
422 nitrogen deposition over the Yellow Sea, and Zhang et al. (2010), who that nitrogen  
423 deposition accounted for 1.1~3.9% of PP over East China Sea.

424 Recently, several studies have evaluated the change of global primary production  
425 under future climate change (Steinacher et al., 2010; Koga et al., 2011; Laufkötter et al.,  
426 2015; Cabré et al., 2015). For instance, based on multi-model ensembles, Cabré et al.  
427 (2015) found a general decrease of total PP projected under RCP 8.5 by the end of this  
428 century. We calculate the seasonal PP from NO<sub>y</sub> using ACCMIP, with results shown in  
429 Fig. 9. Note that PP in Fig. 9 is the equivalent primary production converted from NO<sub>y</sub>  
430 deposited into the ocean through nutrients uptake by phytoplankton. Due to low sea  
431 surface temperature in winter, the conversion can hardly happen and the nutrients may  
432 remain until spring (Reay et al., 1999). Therefore, actual PP from NO<sub>y</sub> may shift from  
433 winter to spring instead. Under RCP scenarios, consistent with the change patterns of  
434 total NO<sub>y</sub> deposition (not shown), PP decreases significantly over the BYE areas in the  
435 2100s, by 60~68% and 34~63% in the four seasons over the Yellow Sea and East China  
436 Sea, respectively, under RCP 8.5 (third and fifth rows in Fig. 9). However, in the 2030s,  
437 PP from NO<sub>y</sub> shows an increase over the BYE areas under RCP 8.5 (e.g., 32~53% in  
438 the Yellow Sea and 19~34% in East China Sea; fourth row in Fig. 9), with smaller



439 increase or decrease under RCP 4.5 (second row in Fig. 9). The large increase of  $\text{NO}_y$   
440 in the near future suggests the increased risk of algal blooms if emission continues to  
441 increase, and the reduction in  $\text{NO}_y$  in 2100 indicates the importance of emission  
442 reduction in the long-term. Without emission reduction, PP from  $\text{NO}_y$  is projected to  
443 increase in 2100 during summer (last row in Fig. 9) over the East China Sea, consistent  
444 with the wet deposition pattern change depicted in Fig. 6, indicating that climate change  
445 increases eutrophication through enhancement of precipitation that increases wet  
446 deposition over this region. Hence our results illustrate the importance of reducing  
447 emissions on PP in the BYE areas in the future.

448  
449



450

451 Fig. 9. Spatial distribution of the percentage change of primary production generated from  $\text{NO}_y$   
452 deposition over east Asia for all scenarios used in this study. Areas over land are blank because the



453 Redfield ratio used is only application to the ocean areas. From the second row, all distributions are  
454 percentage change compared to historical period and only values with agreement are shown. Values  
455 with statistical significance ( $\alpha=0.05$ ) are marked with a black dot.

## 456 7. Conclusions and discussions

457 Atmospheric  $\text{NO}_y$  deposition over East Asia is analyzed to delineate the influence  
458 of climate and emission changes based on the ACCMIP multi-model ensemble. Under  
459 both RCP 4.5 and RCP 8.5 scenarios with combined effect of climate and emission  
460 changes, both dry and wet  $\text{NO}_y$  deposition shows significant decreases in the 2100s,  
461 primarily as a result of large reduction in anthropogenic emissions. In the 2030s, both  
462 the dry and wet  $\text{NO}_y$  deposition increases significantly, particularly under RCP 8.5,  
463 mainly because of enhanced emissions. The individual effect of climate change and  
464 emissions on the dry and wet  $\text{NO}_y$  deposition is also identified, showing relatively  
465 minor impact of climate change on dry  $\text{NO}_y$  deposition. In terms of wet deposition, the  
466 spatial patterns are in general consistent with those in the changes of precipitation,  
467 particularly at the end of this century. Take the East China Sea as an example, wet  $\text{NO}_y$   
468 deposition increases significantly in summer (18%) and decreases significantly in  
469 winter (-13%). While climate change alone generally increases wet deposition,  
470 reduction of emission has a dominant influence of reducing wet deposition over East  
471 China.

472 Over the Chinese coastal seas such as Yellow Sea and East China Sea, with  
473 decreasing transport of  $\text{NO}_x$  from mainland China due to emission reduction, ship and  
474 lightning emissions from the ocean become the major source of  $\text{NO}_y$  deposition, with  
475 mean seasonal increase of 24-48% and 3%-37% for Yellow Sea and East China Sea,  
476 respectively. Therefore, reducing ship emission in the Chinese coastal areas is a key  
477 factor to reduce nitrogen deposition in the future.

478 In the 2030s, PP from  $\text{NO}_y$  shows increases over the BYE areas under RCP 8.5,  
479 suggesting the increased risk of algal blooms if emission such as from ships continues  
480 to increase in the near future (Liu et al., 2016). With climate change only, PP from  $\text{NO}_y$



481 is projected to increase in 2100 during summer over the East China Sea, indicating a  
482 supportive role of climate change on eutrophication, and hence the importance of  
483 emission controls.

484 Although the ACCMIP multi-model ensemble has provided valuable information  
485 for projecting future changes in NO<sub>y</sub> deposition, the models used in ACCMIP have  
486 relatively coarse spatial resolution for resolving the complex meteorological and  
487 chemical processes. Dynamical downscaling may be applied in the future to further  
488 investigate the impact of climate and emission on nitrogen deposition over East Asia  
489 and the detailed processes involved. For analysis of marine primary production, we  
490 used a very simple approach that ignores biogeochemical processes in the ocean. An  
491 ocean biogeochemistry model will be useful to further quantify the effect of climate and  
492 emissions on PP.

493

494

495 **Competing interests.** The authors declare that they have no conflict of interest.

496 **Acknowledgement.** This research was supported by grants from the National Key Project of  
497 MOST (2017YFC1404101), Shandong Provincial Natural Science Foundation, China  
498 (ZR2017MD026) and National Natural Science Foundation of China (41705124, 41822505 and  
499 91544110). PNNL is operated for DOE by Battelle Memorial Institute under contract DE-AC05-  
500 76RL01830.

501

## 502 **References:**

- 503 Adler, R. F., Sapiano, M. R. P., Huffman, G. J., Wang, J. J., Gu, G., Bolvin, D., Long, C., Schneider, U.,  
504 Becker, A., and Nelkin, E.: The Global Precipitation Climatology Project (GPCP) Monthly Analysis  
505 (New Version 2.3) and a Review of 2017 Global Precipitation, *Atmosphere*, 9, 138, 2018.
- 506 Allen, R. J., Landuyt, W., and Rumbold, S. T.: An increase in aerosol burden and radiative effects in a  
507 warmer world, *Nat. Clim. Change*, 6, 2015.
- 508 Baker, A. R., Kanakidou, M., Altieri, K. E., Daskalakis, N., Okin, G. S., Myriokefalitakis, S., Dentener,  
509 F., Uematsu, M., Sarin, M. M., and Duce, R. A.: Observation- and Model-Based Estimates of  
510 Particulate Dry Nitrogen Deposition to the Oceans, *Atmos. Chem. Phys.*, 17, 8189-8210, 2017.
- 511 Butchart, S. H. M., Walpole, M., Collen, B., Strien, A. v., Scharlemann, J. P. W., Almond, R. E. A., Baillie,  
512 J. E. M., Bomhard, B., Brown, C., and Bruno, J.: Global biodiversity: indicators of recent declines,  
513 *Science*, 328, 1164-1168, 2010.
- 514 Cabré, A., Marinov, I., and Leung, S.: Consistent global responses of marine ecosystems to future climate  
515 change across the IPCC AR5 earth system models, *Clim. Dynam.*, 45, 1-28, 2015.



- 516 Chong-Hai, and Ying: The Projection of Temperature and Precipitation over China under RCP Scenarios  
517 using a CMIP5 Multi-Model Ensemble, *Atmos. Ocean. Sci. Lib.*, 5, 527-533, 2012.
- 518 Cong, Z. Y., Kang, S. C., Zhang, Y. L., and Li, X. D.: Atmospheric wet deposition of trace elements to  
519 central Tibetan Plateau, *Appl. Geochem.*, 25, 1415-1421,  
520 <https://doi.org/10.1016/j.apgeochem.2010.06.011>, 2010.
- 521 Connan, O., Maro, D., Hebert, D., Rounsard, P., Goujon, R., Letellier, B., and Le Cavelier, S.: Wet and  
522 dry deposition of particles associated metals (Cd, Pb, Zn, Ni, Hg) in a rural wetland site, Marais  
523 Vernier, France, *Atmos. Environ.*, 67, 394-403, <https://doi.org/10.1016/j.atmosenv.2012.11.029>,  
524 2013.
- 525 Dalsøren, S. B., Eide, M. S., Endresen, and Mjelde, A.: Update on emissions and environmental impacts  
526 from the international fleet of ships. The contribution from major ship types and ports, *Atmos. Chem.*  
527 *Phys.*, 9, 18323-18384, 2009.
- 528 Ding, Y. H.: Monsoons over China, *Atmos.sci.library*, 419, 252-252, 1991.
- 529 Doney, S. C., Mahowald, N., Lima, I., Feely, R. A., Mackenzie, F. T., Lamarque, J.-F., and Rasch, P. J.:  
530 Impact of anthropogenic atmospheric nitrogen and sulfur deposition on ocean acidification and the  
531 inorganic carbon system, *P. Natl. Acad. Sci.*, 104, 14580-14585, 2007.
- 532 Duce, R. A., LaRoche, J., Altieri, K., Arrigo, K. R., Baker, A. R., Capone, D. G., Cornell, S., Dentener,  
533 F., Galloway, J., Ganeshram, R. S., Geider, R. J., Jickells, T., Kuypers, M. M., Langlois, R., Liss, P.  
534 S., Liu, S. M., Middelburg, J. J., Moore, C. M., Nickovic, S., Oeschlies, A., Pedersen, T., Prospero,  
535 J., Schlitzer, R., Seitzinger, S., Sorensen, L. L., Uematsu, M., Ulloa, O., Voss, M., Ward, B., and  
536 Zamora, L.: Impacts of Atmospheric Anthropogenic Nitrogen on the Open Ocean, *Science*, 320,  
537 893-897, <https://doi.org/10.1126/science.1150369>, 2008.
- 538 Ellis, R., Jacob, D. J., Sulprizio, M. P., Zhang, L., Holmes, C., Schichtel, B., Blett, T., Porter, E., Pardo,  
539 L., and Lynch, J.: Present and future nitrogen deposition to national parks in the United States:  
540 critical load exceedances, *Atmos. Chem. Phys.*, 13, 9083-9095, 2013.
- 541 Erisman, J. W., and Draaijers, G.: Deposition to forests in Europe: most important factors influencing  
542 dry deposition and models used for generalisation, *Environ. Pollut.*, 124, 379-388, 2003.
- 543 Eyring, V., Isaksen, I. S., Berntsen, T., Collins, W. J., Corbett, J. J., Endresen, O., Grainger, R. G.,  
544 Moldanova, J., Schlager, H., and Stevenson, D. S.: Transport impacts on atmosphere and climate:  
545 Shipping, *Atmos. Environ.*, 44, 4735-4771, 2010.
- 546 Fan, Q., Zhang, Y., Ma, W., Ma, H., Feng, J., Yu, Q., Yang, X., Ng, S. K., Fu, Q., and Chen, L.: Spatial  
547 and seasonal dynamics of ship emissions over the Yangtze River Delta and East China Sea and their  
548 potential environmental influence, *Environ. Sci. Technol.*, 50, 1322-1329, 2016.
- 549 Galloway, J. N., Townsend, A. R., Erisman, J. W., Bekunda, M., Cai, Z. C., Freney, J. R., Martinelli, L.  
550 A., Seitzinger, S. P., and Sutton, M. A.: Transformation of the nitrogen cycle: Recent trends,  
551 questions, and potential solutions, *Science*, 320, 889-892, <https://doi.org/10.1126/science.1136674>,  
552 2008.
- 553 Gao, Y., Leung, L. R., Lu, J., Liu, Y., Huang, M., and Qian, Y.: Robust spring drying in the southwestern  
554 U.S. and seasonal migration of wet/dry patterns in a warmer climate, *Geophys. Res. Lett.*, 41, 1745-  
555 1751, <https://doi.org/10.1002/2014GL059562>, 2014.
- 556 Gao, Y., Leung, L. R., Lu, J., and Masato, G.: Persistent cold air outbreaks over North America in a  
557 warming climate, *Environ. Res. Lett.*, 10, 044001, 2015.
- 558 Gao, Y., Lu, J., and Leung, L. R.: Uncertainties in Projecting Future Changes in Atmospheric Rivers and  
559 Their Impacts on Heavy Precipitation over Europe, *J. Climate*, 29, 6711-6726,



- 560 <http://dx.doi.org/10.1175/JCLI-D-16-0088.1>, 2016.
- 561 Gong, G. C., Shiah, F. K., Liu, K. K., Wen, Y. H., and Liang, M. H.: Spatial and temporal variation of  
562 chlorophyll a, primary productivity and chemical hydrography in the southern East China Sea, *Cont.*  
563 *Shelf. Res.*, 20, 411-436, 2000.
- 564 Gong, G. C., Wen, Y. H., Wang, B. W., and Liu, G. J.: Seasonal variation of chlorophyll a concentration,  
565 primary production and environmental conditions in the subtropical East China Sea, *Deep-Sea*  
566 *Research Part II*, 50, 1219-1236, 2003.
- 567 Guan, W. J., Xian-Qiang, H. E., Pan, D. L., and Fang, G.: Estimation of ocean primary production by  
568 remote sensing in Bohai Sea, Yellow Sea and East China Sea, *J. Fish. China*, 29, 367-372, 2005.
- 569 Hu, C., Li, D., Chen, C., Ge, J., Muller-Karger, F. E., Liu, J., Yu, F., and He, M. X.: On the recurrent  
570 *Ulva prolifera* blooms in the Yellow Sea and East China Sea, *J. Geophys. Res-Oceans*, 115, 2010.
- 571 Kim, G., Scudlark, J. R., and Church, T. M.: Atmospheric wet deposition of trace elements to Chesapeake  
572 and Delaware Bays, *Atmos. Environ.*, 34, 3437-3444, [https://doi.org/10.1016/S1352-](https://doi.org/10.1016/S1352-2310(99)00371-4)  
573 [2310\(99\)00371-4](https://doi.org/10.1016/S1352-2310(99)00371-4), 2000.
- 574 Kim, J. E., Han, Y. J., Kim, P. R., and Holsen, T. M.: Factors influencing atmospheric wet deposition of  
575 trace elements in rural Korea, *Atmos. Res.*, 116, 185-194,  
576 <https://doi.org/10.1016/j.atmosres.2012.04.013>, 2012.
- 577 Koga, N., Smith, P., Yeluripati, J. B., Shirato, Y., Kimura, S. D., and Nemoto, M.: Estimating net primary  
578 production and annual plant carbon inputs, and modelling future changes in soil carbon stocks in  
579 arable farmlands of northern Japan, *Agr. Ecosys. Environ.*, 144, 51-60, 2011.
- 580 Kryza, M., Werner, M., Dore, A. J., Błaś, M., and Sobik, M.: The role of annual circulation and  
581 precipitation on national scale deposition of atmospheric sulphur and nitrogen compounds, *J.*  
582 *Environ. Manage.*, 109, 70-79, 2012.
- 583 Lamarque, J. F., Kiehl, J. T., Brasseur, G. P., Butler, T., Cameron-Smith, P., Collins, W. D., Collins, W.  
584 J., Granier, C., Hauglustaine, D., Hess, P. G., Holland, E. A., Horowitz, L., Lawrence, M. G.,  
585 McKenna, D., Merilees, P., Prather, M. J., Rasch, P. J., Rotman, D., Shindell, D., and Thornton, P.:  
586 Assessing future nitrogen deposition and carbon cycle feedback using a multimodel approach:  
587 Analysis of nitrogen deposition, *J. Geophys. Res-Atmos.*, 110,  
588 <https://doi.org/10.1029/2005JD005825>, 2005.
- 589 Lamarque, J. F., Dentener, F., McConnell, J., and Ro, C. U.: Multi-model mean nitrogen and sulfur  
590 deposition from the Atmospheric Chemistry and Climate Model Intercomparison Project  
591 (ACCMIP): evaluation historical and projected changes, *Atmos. Chem. Phys.*, 13, 7997-8018,  
592 2013a.
- 593 Lamarque, J. F., Shindell, D. T., Josse, B., Young, P. J., Cionni, I., Eyring, V., Bergmann, D., Cameron-  
594 Smith, P., Collins, W. J., Doherty, R., Dalsoren, S., Faluvegi, G., Folberth, G., Ghan, S. J., Horowitz,  
595 L. W., Lee, Y. H., MacKenzie, I. A., Nagashima, T., Naik, V., Plummer, D., Righi, M., Rumbold, S.,  
596 Schulz, M., Skeie, R. B., Stevenson, D. S., Strode, S., Sudo, K., Szopa, S., Voulgarakis, A., and  
597 Zeng, G.: The Atmospheric Chemistry and Climate Model Intercomparison Project (ACCMIP):  
598 overview and description of models, simulations and climate diagnostics, *Geosci. Model Dev.*, 6,  
599 179-206, <https://doi.org/10.5194/gmd-6-179-2013>, 2013b.
- 600 Laufkötter, C., Vogt, M., Gruber, N., Aitanoguchi, M., Aumont, O., Bopp, L., Buitenhuis, E., Doney, S.  
601 C., Dunne, J., and Hashioka, T.: Drivers and uncertainties of future global marine primary  
602 production in marine ecosystem models, *Biogeosciences Discussions*, 12, 6955-6984, 2015.
- 603 Liu, H., Fu, M., Jin, X., Shang, Y., Shindell, D., Faluvegi, G., Shindell, C., and He, K.: Health and climate



- 604 impacts of ocean-going vessels in East Asia, *Nat. Clim. Change*, 6, 2016.
- 605 Liu, L., Zhang, X., Xu, W., Liu, X., Lu, X., Chen, D., Zhang, X., Wang, S., and Zhang, W.: Estimation  
606 of monthly bulk nitrate deposition in China based on satellite NO<sub>2</sub> measurement by the Ozone  
607 Monitoring Instrument, *Remote Sens. Environ.*, 199, 93-106, 2017.
- 608 Liu, X., Zhang, Y., Han, W., Tang, A., Shen, J., Cui, Z., Vitousek, P., Erisman, J. W., Goulding, K., and  
609 Christie, P.: Enhanced nitrogen deposition over China, *Nature*, 494, 459-462, 2013.
- 610 Luo, X. S., Tang, A. H., Shi, K., Wu, L. H., Li, W. Q., Shi, W. Q., Shi, X. K., Erisman, J. W., Zhang, F.  
611 S., and Liu, X. J.: Chinese coastal seas are facing heavy atmospheric nitrogen deposition, *Environ.*  
612 *Res. Lett.*, 9, 095007, 2014.
- 613 Montoya-Mayor, R., Fernandez-Espinosa, A. J., Seijo-Delgado, I., and Ternero-Rodriguez, M.:  
614 Determination of soluble ultra-trace metals and metalloids in rainwater and atmospheric deposition  
615 fluxes: A 2-year survey and assessment, *Chemosphere*, 92, 882-891,  
616 <https://doi.org/10.1016/j.chemosphere.2013.02.044>, 2013.
- 617 Paerl, and Hans, W.: Coastal eutrophication and harmful algal blooms: Importance of atmospheric  
618 deposition and groundwater as &ldquo;new&rdquo; nitrogen and other nutrient sources, *Limnol.*  
619 *Oceanogr.*, 42, 1154-1165, 1997.
- 620 Paerl, H. W., Dennis, R. L., and Whitall, D. R.: Atmospheric deposition of nitrogen: Implications for  
621 nutrient over-enrichment of coastal waters, *Estuaries*, 25, 677-693, 2002.
- 622 Qi, J. H., Shi, J. H., Gao, H. W., and Sun, Z.: Atmospheric dry and wet deposition of nitrogen species  
623 and its implication for primary productivity in coastal region of the Yellow Sea, China, *Atmos.*  
624 *Environ.*, 81, 600-608, 2013.
- 625 Reay, D. S., Nedwell, D. B., Priddle, J., and Ellis-Evans, J. C.: Temperature dependence of inorganic  
626 nitrogen uptake: reduced affinity for nitrate at suboptimal temperatures in both algae and bacteria,  
627 *Appl. Environ. Microb.*, 65, 2577-2584, 1999.
- 628 Reichler, T., and Kim, J.: How well do coupled models simulate today's climate?, *B. Am. Meteorol. Soc.*,  
629 89, 303-311, <https://doi.org/10.1175/Bams-89-3-303>, 2008.
- 630 Shindell, D. T., Lamarque, J. F., Schulz, M., Flanner, M., Jiao, C., Chin, M., Young, P. J., Lee, Y. H.,  
631 Rotstain, L., Mahowald, N., Milly, G., Faluvegi, G., Balkanski, Y., Collins, W. J., Conley, A. J.,  
632 Dalsoren, S., Easter, R., Ghan, S., Horowitz, L., Liu, X., Myhre, G., Nagashima, T., Naik, V.,  
633 Rumbold, S. T., Skeie, R., Sudo, K., Szopa, S., Takemura, T., Voulgarakis, A., Yoon, J. H., and Lo,  
634 F.: Radiative forcing in the ACCMIP historical and future climate simulations, *Atmos. Chem. Phys.*,  
635 13, 2939-2974, <https://doi.org/10.5194/acp-13-2939-2013>, 2013.
- 636 Son, S., Campbell, J., Dowell, M., Yoo, S., and Noh, J.: Primary production in the Yellow Sea determined  
637 by ocean color remote sensing, *Mar. Ecol.-Prog. Ser.*, 303, 91-103, 2005.
- 638 Steinacher, M., Joos, F., Frölicher, T. L., Bopp, L., Cadule, P., Cocco, V., Doney, S. C., Gehlen, M.,  
639 Lindsay, K., and Moore, J. K.: Projected 21st century decrease in marine productivity: a multi-  
640 model analysis, *Biogeosciences*, 7, 979-1005, 2010.
- 641 Steinfeld, J.: Atmospheric Chemistry and Physics: From Air Pollution to Climate Change, *Environ. Sci.*  
642 *Policy Sustainable Dev.*, 40, 26-26, 1998.
- 643 Stevens, C. J., Lind, E. M., Hautier, Y., Harpole, W. S., Borer, E. T., Hobbie, S., Seabloom, E. W., Ladwig,  
644 L., Bakker, J. D., Chu, C. J., Collins, S., Davies, K. F., Firm, J., Hillebrand, H., La Pierre, K. J.,  
645 MacDougall, A., Melbourne, B., McCulley, R. L., Morgan, J., Orrock, J. L., Prober, S. M., Risch,  
646 A. C., Schuetz, M., and Wragg, P. D.: Anthropogenic nitrogen deposition predicts local grassland  
647 primary production worldwide, *Ecology*, 96, 1459-1465, 2015.



- 648 Tett, P., Droop, M. R., and Heaney, S. I.: The Redfield Ratio and Phytoplankton Growth Rate, *J. Mar.*  
649 *Biol. Assoc. UK*, 65, 487-504, 1985.
- 650 Theodosi, C., Markaki, Z., Tselepidis, A., and Mihalopoulos, N.: The significance of atmospheric inputs  
651 of soluble and particulate major and trace metals to the eastern Mediterranean seawater, *Mar. Chem.*,  
652 120, 154-163, <https://doi.org/10.1016/j.marchem.2010.02.003>, 2010.
- 653 Van Vuuren, D. P., Edmonds, J., Kainuma, M., Riahi, K., Thomson, A., Hibbard, K., Hurtt, G. C., Kram,  
654 T., Krey, V., and Lamarque, J.-F.: The representative concentration pathways: an overview, *Climatic*  
655 *Change*, 109, 5, 2011.
- 656 Vuai, S. A. H., and Tokuyama, A.: Trend of trace metals in precipitation around Okinawa Island, Japan,  
657 *Atmos. Res.*, 99, 80-84, <https://doi.org/10.1016/j.atmosres.2010.09.010>, 2011.
- 658 Wałaszek, K., Kryza, M., and J. Dore, A.: The impact of precipitation on wet deposition of sulphur and  
659 nitrogen compounds, *Ecol. Chem. Eng. S.*, 20, 733-745, <https://doi.org/10.2478/eces-2013-0051>,  
660 2013.
- 661 Wang, L., and Chen, W.: A CMIP5 multimodel projection of future temperature, precipitation, and  
662 climatological drought in China, *Int. J. Climatol.*, 34, 2059-2078, 2014.
- 663 Wang, Y., Zhang, Q., He, K., Zhang, Q., and Chai, L.: Sulfate-nitrate-ammonium aerosols over China:  
664 response to 2000–2015 emission changes of sulfur dioxide, nitrogen oxides, and ammonia, *Atmos.*  
665 *Chem. Phys.*, 13, 2635-2652, 2013.
- 666 Xu, W., Liu, L., Cheng, M., Zhao, Y., Zhang, L., Pan, Y., Zhang, X., Gu, B., Li, Y., Zhang, X., Shen, J.,  
667 Lu, L., Luo, X., Zhao, Y., Feng, Z., Collett Jr, J. L., Zhang, F., and Liu, X.: Spatial-temporal patterns  
668 of inorganic nitrogen air concentrations and deposition in eastern China, *Atmos. Chem. Phys.*, 18,  
669 10931-10954, <https://doi.org/10.5194/acp-18-10931-2018>, 2018.
- 670 Zhang, X. Y., Lu, X. H., Liu, L., Chen, D. M., Zhang, X. M., Liu, X. J., and Zhang, Y.: Dry deposition of  
671 NO<sub>2</sub> over China inferred from OMI columnar NO<sub>2</sub> and atmospheric chemistry transport model,  
672 *Atmos. Environ.*, 169, 2017.
- 673 Zhang, Y., Yu, Q., Ma, W., and Chen, L.: Atmospheric deposition of inorganic nitrogen to the eastern  
674 China seas and its implications to marine biogeochemistry, *J. Geophys. Res-Atmos.*, 115, 2010.  
675